

A Combined Analytical-Numerical Methodology for Predicting Subharmonic Oscillation in H-Bridge Inverters Under Double Edge Modulation

Abdelali El Aroudi¹, *Senior Member, IEEE*, Mohammed S. Al-Numay, *Member, IEEE*,

Wei Guo Lu², *Member, IEEE*, Josep Maria Bosque-Moncusí,

and Herbert Ho-Ching Iu³, *Senior Member, IEEE*

Abstract—In this paper, a combined analytical-numerical methodology is developed for detecting subharmonic oscillation in H-bridge inverters with an LC filter and under double edge modulation. The prediction of this phenomenon is accomplished accurately by combining analytical expressions and computational procedures to determine the switching instants and the corresponding periodic orbits. Different approximate closed-form expressions for the stability boundary are derived revealing the effect of the parameters of the system on its dynamical behavior and showing that the stability boundary is different from the ones corresponding to single edge modulation strategies such as trailing edge and leading edge modulations. The theoretical results are validated by numerical simulations using a system-level switched model. Also, a prototype is implemented to validate the theoretical derivations and the numerical simulations getting a good matching.

Index Terms—Switching converters, H-bridge inverters, double edge modulation, subharmonic oscillation.

I. INTRODUCTION

SUBHARMONIC instability in switched mode power converters has increasingly attracted the interest of many researchers during the last couple of decades [1]–[3]. A significant amount of knowledge has been reached about the occurrence of this phenomenon in these systems under both Current Mode Control (CMC) and Voltage Mode Control (VMC) [4]–[8]. Most of the previous studies consider

dc-dc converters under single edge modulation schemes such as Trailing Edge Modulation (TEM) and Leading Edge Modulation (LEM). Trailing-edge modulation is most common in dc-dc converters. However, Double Edge Modulation (DEM) is used in many applications involving H-bridge structures. For instance, in dc-ac and ac-dc energy conversion, this modulation strategy eliminates certain harmonics when the reference is a sine wave [9, Ch. 3].

With the ever-increasing development of the renewable energy technology, dc-ac inverters become one of the most attractive and viable solutions to the power conversion problem. They have been extensively used in various actual applications and are playing key roles in renewable energy integration [10], [11]. They are also used in motor drive [12], [13] and DSTATCOM applications [14] as well as in many uninterruptible power supply system applications such as plant facilities and factories, medical equipments and centers in hospitals, airline computer and communication systems in server farms and web hosting sites [15].

In stand-alone operation mode, the load is directly supplied by the inverter. Single-phase H-bridge inverters are simple bidirectional converter topologies capable of handling both real and reactive power having their performance evaluated in terms of power quality and stability. Therefore, generating a high quality output voltage with low distortion and good voltage regulation is the main target. Other relevant performance metrics include disturbance rejection, transient response, and insensitivity to load and system parameter variations. These metrics can only be achieved with a design free from any kind of instability. Namely, when subharmonic oscillation takes place in a switched mode power converter, usually the ripple in the currents and voltages increases and this has a harmful effect on the system performances since the overall losses become more significant. In dc-ac inverters, the power quality is also jeopardized since the subharmonic oscillation increases the THD and the current stress on the switches. Therefore, the prediction of this phenomenon is of high importance from both theoretical and practical point of view and remains an important research topic.

Accurate modeling and stability analysis are necessary for exploring the dynamic behavior and predicting the stability boundaries of dc-ac H-bridge inverters. The first and direct

Manuscript received July 11, 2017; revised September 20, 2017 and October 29, 2017; accepted December 1, 2017. This work was supported by the Spanish Ministerio de Economía y Competitividad under Grant DPI2013-47293-R. The work of A. E. Aroudi and M. S. Al-Numay was supported by the International Scientific Partnership Program ISPP, King Saud University, through ISPP under Grant 00102. This paper was recommended by Associate Editor K.-H. Chen. (*Corresponding author: Abdelali El Aroudi.*)

A. E. Aroudi and J. M. Bosque-Moncusí are with the GAEI Research Group, Department d'Enginyeria Electrònica, Elèctrica i Automàtica, Universitat Rovira i Virgili, 43007 Tarragona, Spain (e-mail: abdelali.elaroudi@urv.cat).

M. S. Al-Numay is with the Electrical Engineering Department, King Saud University, Riyadh 11421, Saudi Arabia (e-mail: alnumay@ksu.edu.sa).

W. G. Lu is with the State Key Laboratory of Power Transmission Equipment and System Security and New Technology, University of Chongqing, Chongqing 400044, China (e-mail: luweiguo@cqu.edu.cn).

H. H.-C. Iu is with the School of Electrical, Electronic and Computer Engineering, The University of Western Australia, Crawley, WA 6009, Australia (e-mail: herbert.iu@uwa.edu.au).

Color versions of one or more of the figures in this paper are available online at <http://ieeexplore.ieee.org>.

Digital Object Identifier 10.1109/TCSI.2017.2780318

TABLE I

EXISTING RESEARCHES ON PREDICTING SUBHARMONIC OSCILLATION WITH DIFFERENT CONTROL METHODS AND MODULATION STRATEGIES

Control method	Modulation strategy	Approach	Instability condition	Past works
Analog VMC	TEM/LEM	Numerical	Yes	[5], [7], [8]
Digital CMC	DEM	Analytical	Yes	[2]
Analog VMC	DEM	Numerical	No	[19]–[21]
Analog VMC	DEM	Analytical	Eqs. (14) and (18)	This work

approach that one can use is long time transient simulation from detailed switched models. This approach, although very accurate, is very time consuming and can be problematic in some particular applications where repeated long simulations are required. State-space averaging [16], [17] and generalized state space averaging (GSSA) techniques [18] can significantly reduce the simulation time but the models derived from these approaches are unable to predict the actual behavior of the system. In particular, such models are incapable of predicting the occurrence of subharmonic oscillation.

Early researches on subharmonic instability for dc-ac inverters with DEM have been reported in [2], [3], [19], and [20]. In [2] and [3] the dynamics of the output capacitor voltage has been overlooked and only the inductor current was considered as a state variable. In [19] and [20] the complete system has been analyzed but the analytical results concerning stability have been reported only for the slow scale low frequency instabilities using an averaged model. In dc-ac inverters, subharmonic oscillation is a type of local instability which manifests itself as a period-doubling bifurcation in some intervals of a line cycle [19], [20]. In past works subharmonic oscillation in dc-ac inverters has been merely verified by means of numerical simulations using either a discrete-time model or a switched system-level model obtaining the critical phase angle during the line cycle at which subharmonic oscillation is exhibited [19], [20]. Another attempt to study subharmonic oscillation in a dc-dc buck converter with DEM is in [21]. Apart from the preliminary efforts in [20] and [22], closed-form expressions for predicting subharmonic oscillation boundary in H-bridge inverters under DEM have not been reported to the best of authors knowledge. A summary of the different existing researches on predicting subharmonic oscillation in switching converters with different control methods and modulation strategies is given in Table I.

The main contribution of this paper is to develop a methodology for *analytically* determining the boundary of subharmonic oscillation in an H-bridge inverter under DEM strategy for both dc and ac loads. Hence, the stability region in terms of the different system parameters is located. Numerical and experimental results are provided to verify the analytical results. It should be noted that this paper deals with subharmonic oscillation which is a fast scale instability taking place at the switching scale and does not deal with slow scale phenomena that can be tackled by averaged models. It should also be noted that in order to simplify the analysis, only a linear and resistive load was considered and that propagation delay has been ignored. Such effects of load nonlinearities and communication delays like those considered [23] can slightly alter the results obtained in this paper. The complete analysis

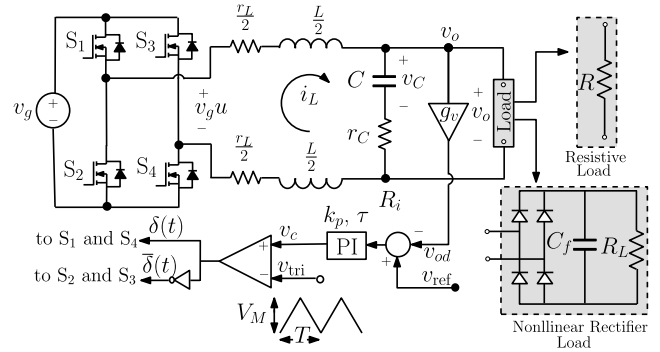


Fig. 1. Circuit diagram of an H-bridge converter with different load types.

taking into account these effects is however considered out of the scope of our work and will be studied in future works. In particular, we will demonstrate that although the original results reported in [20] and [22] are not exact, they lead to a good estimate for the stability boundary of dc-dc converters and dc-ac inverters under the DEM strategy. The results also show that the stability boundary corresponding to the DEM strategy is different from the ones corresponding to single edge modulation strategies such as TEM and LEM. In particular, the stability region corresponding to the DEM strategy is wider. The theoretical results will be validated by numerical simulations from the detailed switched model.

The rest of this paper is organized as follows: Section II presents a brief description of the H-bridge inverter and its mathematical modeling. Stability analysis is performed in Section III using Floquet theory. Different approximate closed-form expressions for the stability boundary are derived in Section IV using the system state-space model. In Section V, time-domain numerical simulations are performed to validate the derived theoretical expressions. An experimental validation is provided in Section VI using a laboratory prototype. Finally, in the last section, some concluding remarks of this work and some perspectives for future works are summarized.

II. SYSTEM DESCRIPTION AND MODELING

The schematic diagram of a dc-ac H-bridge inverter with DEM and a PI voltage mode control is shown in Fig. 1. The basic function of such a system is to convert the voltage of a dc source such as a PV panel or a battery to a sinusoidal ac output through an LC filter and an appropriate action of the inverter switches. For practical reasons related to noise issues, the total inductance L is distributed between the top side and the bottom side of the LC filter. The activation of the switches S_i ($i = 1, \dots, 4$) is carried out as follows: the

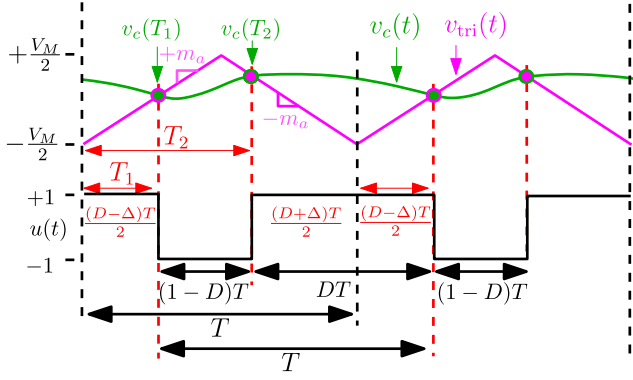


Fig. 2. Waveforms of the double edge PWM signals in T -periodic regime.

output voltage v_o is sensed using a voltage divider with gain g_v to obtain the voltage v_{od} and the voltage error represented by the difference voltage $v_{ref} - v_{od}$ is processed by means of a voltage controller in the form of a PI corrector, where v_{ref} is a voltage reference. The output v_c of this controller is connected to the non-inverting pin of the comparator whereas a symmetric triangular (double edge) signal is applied to the inverting pin, in such a way that the switches S_1 and S_4 are ON (therefore $\delta_1 = \delta_4 = 1$) when $v_c > v_{tri}$ and they are turned OFF when $v_c < v_{tri}$ ($\delta_1 = \delta_4 = 0$). S_2 and S_3 are driven complementarily to S_1 and S_4 respectively. Let $\delta = \delta_1 = \delta_4$ and $\delta_2 = \delta_3 = \bar{\delta} = 1 - \delta$ and D be their steady-state duty cycle. The signal $u(t) = 2\delta - 1$ is defined in such a way that $v_g u$ represents the inverter bridge voltage which is a square wave signal with the same steady-state duty cycle D as the signal u . The load can be either a linear resistive load R or a nonlinear rectifier load including a linear resistance load R_L and nonlinear rectifier. In the last case, the load can be modeled in different levels of complexity depending on the phenomena to be studied. A model based on the first harmonic approximation can be used to show that the effective resistance to represent the effect of the rectifier and load R_L is $R = 8\pi^2/R_L$ [24, Ch. 19].

Fig. 2 shows a sketch of the waveforms of the control signals when the system works in the stable periodic regime. The triangular signal can be expressed during one complete period of length T as follows

$$v_{tri}(t) = \begin{cases} -\frac{V_M}{2} + m_a t & \text{if } 0 \leq t \leq \frac{T}{2} \\ -\frac{V_M}{2} + m_a(T - t) & \text{if } \frac{T}{2} \leq t \leq T \end{cases} \quad (1)$$

where $m_a = 2V_M/T$ represents the raising slope of the triangular signal $v_{tri}(t)$. The state-space model for the dc-ac H-bridge inverter can be expressed as follows

$$\dot{\mathbf{x}} = \mathbf{A}\mathbf{x} + \mathbf{B}u \quad (2a)$$

$$\dot{v}_i = v_{ref} - v_{od} \quad (2b)$$

$$v_o = \mathbf{C}^T \mathbf{x} \quad (2c)$$

where $v_{od} = g_v v_o = g_v \mathbf{C}^T \mathbf{x}$ is the signal from the voltage divider, v_i is the integral of the error voltage $v_{ref} - v_{od}$ and

\mathbf{A} , \mathbf{B} and \mathbf{C} are given by

$$\mathbf{A} = \begin{pmatrix} -\frac{\alpha}{RC} & \frac{\alpha}{C} \\ -\frac{\alpha}{L} & -\frac{\alpha r_C + r_L}{L} \end{pmatrix}, \quad \mathbf{B} = \begin{pmatrix} 0 \\ v_g \end{pmatrix}, \quad (3)$$

$$\mathbf{C} = \alpha \begin{pmatrix} 1 \\ r_C \end{pmatrix}$$

L is the total inductance of the inductor whose dc resistance is r_L , C is the capacitance of the output capacitor, r_C is its Equivalent Series Resistance (ESR), v_g is the input voltage, R is the effective load resistance and $\alpha = R/(R + r_C)$. $\mathbf{x}(t)$ is the vector of the state variables corresponding to the power stage (capacitor voltage v_C and inductor current i_L). As an extra state variable we consider the variable $v_i(t) = \int_{-\infty}^t (v_{ref} - g_v \mathbf{C}^T \mathbf{x}(\zeta)) d\zeta$ corresponding to the integral of the error. The control voltage v_c can be expressed as follows

$$v_c = k_p (v_{ref} - g_v \mathbf{C}^T \mathbf{x}) + W_i v_i \quad (4)$$

where W_i and k_p are the integral and the proportional gains of the PI controller.

III. STABILITY ANALYSIS OF PERIODIC ORBITS

A. The Case of Constant Voltage Reference v_{ref}

Under DEM, as shown in Fig. 2, a symmetric triangle wave is used. The periodic state variables comprise transitions through two different configurations during three subintervals. The values of time instants at which the system switches from one configuration to another are to be determined from the following switching condition

$$v_c\left(\frac{(D - \Delta)T}{2}\right) - v_{tri}\left(\frac{(D - \Delta)T}{2}\right). \quad (5)$$

In particular, the time duration Δ can be determined by solving (5) numerically using (1) and (4). The integral action will force the average value of v_{od} over one switching period to be equal to v_{ref} and hence the average output voltage over the same period V_o to be equal to v_{ref}/g_v in steady-state. By performing a net volt-second balance [24], the steady-state duty cycle can be expressed as follows

$$D = \frac{1}{2} + \frac{V_o(\alpha(R + r_C) + r_L)}{2v_g \alpha(R + r_C)} \quad (6)$$

Subharmonic oscillations occur when such a periodic orbit loses stability. The information about the stability of a periodic orbit is contained in the state transition matrix computed over a complete cycle. The periodic orbit in continuous time is represented by the fixed point ($\mathbf{x}(0) = \mathbf{x}(T)$) in the map obtained by sampling the state in synchronism with the T -periodic triangular signal. The state transition matrix computed over a complete cycle is the monodromy matrix of the map computed at the fixed point. The periodic orbit becomes unstable when any one of the eigenvalue of the matrix \mathbf{M} goes out of the unit circle. According to the Filippov approach [1], the monodromy matrix can be calculated as a product of the state transition matrices across each subsystem and the state transition matrices across the switching events called saltation matrices \mathbf{S}_+^+ and \mathbf{S}_+^- for transition from the

subsystem with $u = -1$ to the subsystem characterized by $u = 1$ and vice versa. Thus, an orbit that goes through the two subsystems corresponding to $u = 1$ and $u = -1$ respectively, the monodromy matrix is given by

$$\mathbf{M} = e^{\mathbf{A}_a \frac{(D+\Delta)T}{2}} \cdot \mathbf{S}_-^+ \cdot e^{\mathbf{A}_a(1-D)T} \cdot \mathbf{S}_+^- \cdot e^{\mathbf{A}_a \frac{(D-\Delta)T}{2}} \quad (7)$$

where \mathbf{A}_a is the augmented state matrix by taking into account the extra state equation (2b). The saltation matrices across switching events are as follows

$$\mathbf{S}_-^+ = \mathbf{I} + \frac{2\mathbf{B}\mathbf{n}^\top}{\dot{v}_c(T_2^-) - m_a}, \quad T_2 = \left(1 - \frac{D + \Delta}{2}\right)T \quad (8a)$$

$$\mathbf{S}_+^- = \mathbf{I} - \frac{2\mathbf{B}\mathbf{n}^\top}{\dot{v}_c(T_1^-) + m_a}, \quad T_1 = \frac{D - \Delta}{2}T \quad (8b)$$

where $\mathbf{n} = g_v \mathbf{C}$ is the vector of the feedback coefficients and \mathbf{I} is the identity matrix with appropriate dimension. The terms $\dot{v}_c(T_1^-)$ and $\dot{v}_c(T_2^-)$ are the time derivatives of the control voltage v_c at time instant just before T_1 and T_2 respectively within a switching cycle and they can be expressed as follows

$$\dot{v}_c(T_2^-) = k_p \dot{v}_{\text{ref}} - \mathbf{n}^\top (\mathbf{A}\mathbf{x}(T_2) + \mathbf{B}) + W_i \dot{v}_i(T_2) \quad (9a)$$

$$\dot{v}_c(T_1^-) = k_p \dot{v}_{\text{ref}} - \mathbf{n}^\top (\mathbf{A}\mathbf{x}(T_1) - \mathbf{B}) + W_i \dot{v}_i(T_1) \quad (9b)$$

where \dot{v}_{ref} is the time derivative of the reference signal v_{ref} . The terms $\mathbf{x}(T_1)$ and $\mathbf{x}(T_2)$ in (9a)-(9b) are needed to compute the slopes of the control voltage v_c at time instants just before the switching instants T_1 and T_2 and these slopes in turn are needed to compute the saltation matrices in (8a)-(8b). These terms can be obtained by imposing periodicity during a switching cycle and are given by:

$$\mathbf{x}(T_1) = (\mathbf{I} - e^{\mathbf{A}T})^{-1} [e^{\mathbf{A}DT} \mathbf{A}^{-1} (e^{\mathbf{A}(1-D)T} - \mathbf{I}) + \mathbf{A}^{-1} (e^{\mathbf{A}DT} - \mathbf{I})] \mathbf{B} \quad (10a)$$

$$\mathbf{x}(T_2) = (\mathbf{I} - e^{\mathbf{A}T})^{-1} [e^{\mathbf{A}(1-D)T} \mathbf{A}^{-1} (e^{\mathbf{A}DT} - \mathbf{I}) + \mathbf{A}^{-1} (e^{\mathbf{A}(1-D)T} - \mathbf{I})] \mathbf{B} \quad (10b)$$

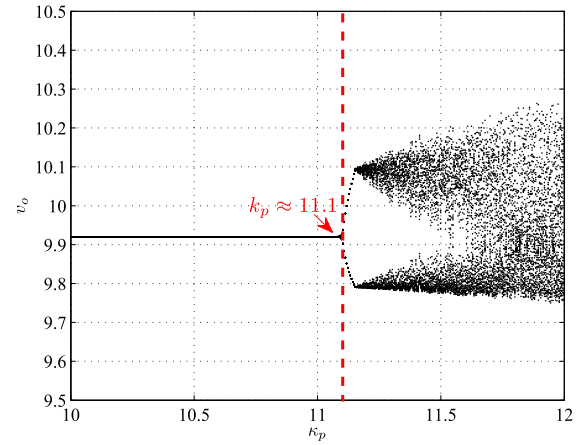
According to (2b), the values of $\dot{v}_i(T_1)$ and $\dot{v}_i(T_2)$ in (9a) and (9b) are as follows

$$\dot{v}_i(T_1) = v_{\text{ref}} - \mathbf{n}^\top \mathbf{x}(T_1), \quad \dot{v}_i(T_2) = v_{\text{ref}} - \mathbf{n}^\top \mathbf{x}(T_2) \quad (11)$$

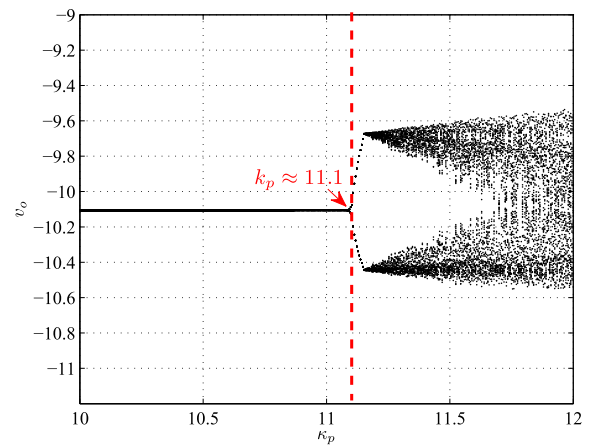
Once a periodic orbit is located, its stability analysis can be performed by using the expression of the monodromy matrix \mathbf{M} given in (7).

Remark 1: One can note that the monodromy matrix is invariant when changing the stationary duty cycle D by its complementary $1 - D$. Hence, it is expected that the same stability status will be obtained for the system for two complementary values of the steady-state duty cycle D .

To confirm the previous remark, different numerical simulations are performed. First, bifurcation diagrams with two complementary values of the steady-state duty cycle are computed by varying the proportional gain k_p in the range (10, 12). Long time integration from the switched model implemented in PSIM[®] was used to obtain the bifurcation diagrams for $D = 0.755$ and $D = 0.245$ and the results are depicted in Fig. 3. These show that the same bifurcation patterns are obtained and that the system undergoes period doubling at the same value of the proportional gain k_p . According to Fig. 3, the critical value



(a)



(b)

Fig. 3. Bifurcation diagrams when k_p is varied for two different but symmetric values of the steady-state duty cycle D . (a) $D = 0.755$ ($V_o = 10$ V). (b) $D = 0.245$ ($V_o = -10$ V).

TABLE II

THE USED PARAMETER VALUES FOR THE INVERTER

L, r_L	C, r_C	V_M	V_g	τ	f_s	R	g_v
660 μ H, 0.2 Ω	68 μ F, 0.1 Ω	2 V	20 V	1 ms	10 kHz	10 Ω	$\frac{1}{7}$

of this parameter is $k_p \approx 11.2$. Second, eigenvalues analysis was performed using Floquet theory and the expression of the monodromy matrix and the results are depicted in Fig. 4 for the same previous two complementary values of the steady-state duty cycle by varying the proportional gain k_p in the same range. It can be observed that the critical values for losing stability are practically the same. The values of the fixed parameters used are depicted in Table II. The eigenvalues of the monodromy matrix make the same loci for both values of D as the proportional gain is varied.

IV. APPROXIMATE ANALYTICAL EXPRESSIONS FOR STABILITY BOUNDARY

At a point where subharmonic oscillation is born, one of the eigenvalues of the monodromy matrix is equal to -1 . Because the characteristic equation is $\det(\mathbf{M} - \lambda \mathbf{I}) = 0$, at the boundary

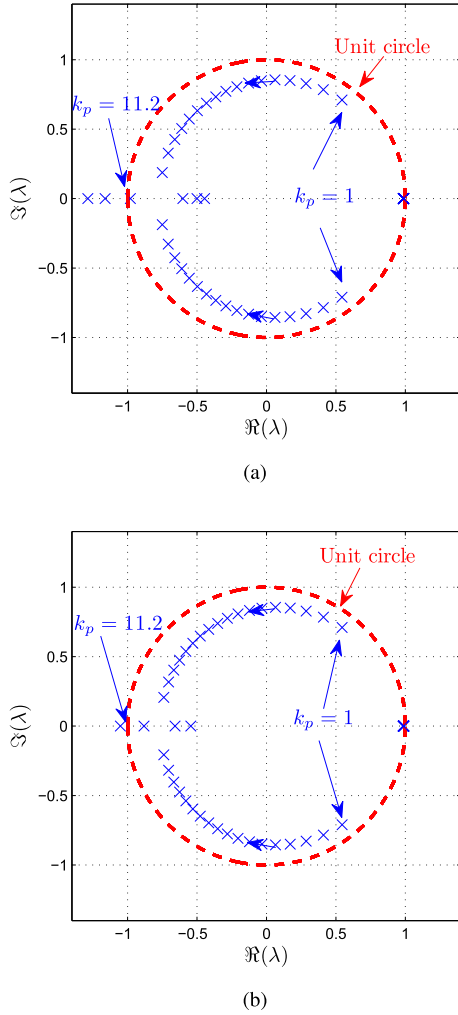


Fig. 4. Eigenvalues loci when k_p is varied for two different but symmetric values of the steady-state duty cycle D . (a) $D = 0.755$ ($V_o = 10$ V). (b) $D = 0.245$ ($V_o = -10$ V).

of subharmonic oscillation, the following condition is fulfilled

$$\det(\mathbf{M} + \mathbf{I}) = 0 \quad (12)$$

The previous equation can be solved numerically to accurately locate the stability boundary of the system in terms of system parameters. Instead of attempting a fully numerical solution for the stability boundary, it is better to solve the problem as thoroughly as possible via analytical techniques. An approximate expression for locating the stability boundary corresponding to the H-bridge inverter under DEM will be derived and will also be contrasted in front of the results obtained from (12) as well as against those computed from the analytical expressions corresponding to TEM and LEM derived in [5] and [8]. Assuming $\Delta = 0$ and $D > 0.5$, it was demonstrated in [20], that a condition for subharmonic oscillation occurrence in a dc-ac inverter under DEM strategy is given by the following Fourier-series-based expression

$$m_a = T \sum_{k=-\infty}^{\infty} (e^{2j\pi(k-\frac{1}{2})D} - 1) H(j(k-\frac{1}{2})\frac{2\pi}{T}) + T \sum_{k=-\infty}^{\infty} (1 - e^{2jk\pi D}) H(jk\frac{2\pi}{T}) \quad (13)$$

where H is the u -to- v_c loop gain of the system. Using well-known properties of Fourier series such as convolution and modulation properties (see [5] for more details) one can demonstrate that the frequency domain condition (13) can be transformed to the following closed-form matrix-form condition

$$m_a = k_p \mathbf{n}^T \left[(\mathbf{I} - e^{ADT})(\mathbf{I} - e^{AT})^{-1} + (\mathbf{I} - e^{-ADT})(\mathbf{I} + e^{AT})^{-1} \right] \mathbf{B} + M_I \quad (14)$$

where M_I is given by

$$M_I = \frac{W_i}{2} (v_{\text{ref}} - \mathbf{n}^T \mathbf{x}(\frac{DT}{2})) = \frac{W_i}{2} (v_{\text{ref}} - v_{od}(\frac{DT}{2})) \quad (15)$$

This term, which shows the effect of the integral action on the subharmonic oscillation boundary, is proportional to the error between v_{ref} and the signal v_{od} from the voltage divider at time instant $DT/2$. For $D < 0.5$ the same condition (14) applies but replacing D with $1 - D$ and T_1 with $T_2 - T/2$. The steady-state periodic orbit at this instant can be obtained by forcing the state vector $\mathbf{x}((D/2 + 1)T)$ after a complete switching cycle to be equal to the initial state $\mathbf{x}(DT/2)$ hence:

$$\mathbf{x}(\frac{DT}{2}) = \mathbf{A}^{-1}(\mathbf{I} - e^{AT})^{-1}(e^{AT} - 2e^{A(1-D)T} + \mathbf{I})\mathbf{B} \quad (16)$$

Remark 2: Note that the matrix $(\mathbf{I} - e^{AT})$ is nonsingular. Note also that if the integral variable was included in the state vector \mathbf{x} this matrix will be singular. The separation of the integral variable from the rest of the state variables avoid many matrix singularities when calculating the stability boundary of the system [8].

The output voltage ripple in the presence of an ESR in the output capacitor can be approximated as follows [24]

$$\Delta v_o \approx \frac{T}{L} \left(\frac{T}{8C} + r_C \right) v_g (1 - D) D \quad (17)$$

Due to the fact that in any practical design $T^2 \ll LC$ and $Tr_C \ll L$, the ripple Δv_o is very small and since $v_{\text{ref}} - v_{od}(DT/2) \leq \Delta v_o$, $v_{\text{ref}} - v_{od}(DT/2)$ is also very small and the term M_I can be ignored without a significant alteration of the results as it will be shown later. Therefore, ignoring M_I , the boundary of subharmonic oscillation is given by the following condition

$$T k_p \mathbf{n}^T [(\mathbf{I} - e^{ADT})(\mathbf{I} - e^{AT})^{-1} + (\mathbf{I} - e^{-ADT})(\mathbf{I} + e^{AT})^{-1}] \mathbf{B} - V_M = 0 \quad (18)$$

According to **Remark 1**, the same expression applies for the case of $D < 0.5$ by changing D with its complementary $1 - D$. In a practical design of an H-bridge inverter, it is desirable that the state variables exhibit stable oscillation for all values of the duty cycle. Based on this concept, stability limit can be determined at the maximum or the minimum value of D in the operating region. By considering the extremum values $D = 1$ or $D = 0$, one has from (18)

$$T k_{p,\text{max}} \mathbf{C}^T [(\mathbf{I} - e^{AT})(\mathbf{I} - e^{AT})^{-1} + (\mathbf{I} - e^{-AT})(\mathbf{I} + e^{AT})^{-1}] \mathbf{B} - V_M = 0 \quad (19)$$

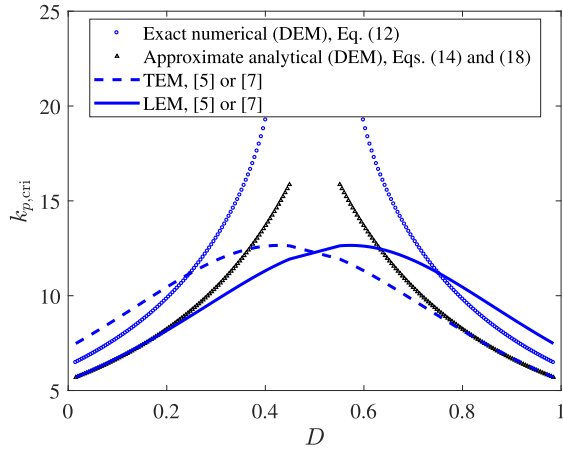


Fig. 5. Stability boundary of the dc-ac H-bridge inverter in terms of the steady-state duty cycle and the PI controller proportional gain. $V_M = 2$ V.

The value of $k_{p,\max}$ can be obtained by solving (19). If the magnitude of the eigenvalues of the matrix \mathbf{A} are much smaller than the switching frequency, as it is the case in switching converters, (18) can be approximated by a polynomial function in terms of D as follows

$$k_p \mathbf{C}^T (\mathbf{I}DT + \frac{1}{2}\mathbf{A}D^2T^2 + \frac{1}{6}\mathbf{A}^2(D^3 - 3D^2 - D)T^3) \mathbf{B} - V_M = 0 \quad (20)$$

By considering the values $D = 1$ or $D = 0$, one obtains

$$k_{p,\max} \mathbf{C}^T (\mathbf{I}T + \frac{1}{2}\mathbf{A}T^2 + \frac{1}{2}\mathbf{A}^2T^3) \mathbf{B} - V_M = 0 \quad (21)$$

Expressing the matrices in (21) leads to

$$\frac{k_{p,\max}}{2LC} \left(T^2 g_v v_g \left(1 + \frac{T}{RC} \right) \right) - V_M = 0 \quad (22)$$

This expression gives an accurate, but conservative, assessment of critical stability limit and does capture the effect of all the parameters upon this limit. This gives an easy and a useful way to select dc-ac H-bridge inverter parameters for guaranteeing a system response free from subharmonic oscillation during all the line cycle. In the sequel, the validity of the derived expressions will be confirmed by numerical simulations and experimental results using an example of H-bridge dc-ac inverter with a DEM strategy.

Using the parameter values shown in Table II, the stability boundary corresponding of the H-bridge inverter under DEM strategy is depicted in Fig. 5. The boundaries corresponding to the TEM and the LEM strategies from [5] are also shown in the same plot demonstrating that different modulation strategies lead to different stability boundaries. For the DEM case, the boundary obtained by ignoring the term M_I is also plotted but its corresponding curve is practically identical to the case when M_I is included. The results show that except in the vicinity of $D = 0.5$, the closed-form expression (18) is accurate enough in a wide range of system parameter values. According to the conservative expression (22), the expression at the extremum values of the steady-state duty cycle gives $k_{p,\max} \approx 2.75$.

A. The Case of Sinusoidal Voltage Reference v_{ref}

In dc-ac applications, the reference voltage is varied sinusoidally as follows: $v_{\text{ref}} = V_{\text{ref}} \sin(\omega_l t)$, where V_{ref} is the peak value of the reference signal. In practice, the switching period is much smaller than the line period and a quasi-static approximation can be used. Let $\phi = \omega_l t$. Therefore, from (6) and using this approximation, the quasi-static duty cycle D_ϕ can be seen as a sinusoidally varying signal according to the following expression:

$$D_\phi = \frac{1}{2} + \frac{V_{\text{ref}}(\alpha(R + r_C) + r_L) \sin(\phi)}{2g_v v_g \alpha(R + r_C)} \quad (23)$$

Hence, for a slowly varying voltage reference, the condition (18) for stability boundary is still valid for dc-ac H-bridge inverters with sinusoidal output after substituting the constant steady-state duty cycle D from (6) by the time-varying duty cycle D_ϕ given in (23).

V. PSIM[®] NUMERICAL SIMULATIONS

In order to validate the theoretical results concerning the stability boundaries, time-domain numerical simulations have been performed using the detailed switched model of the H-bridge inverter implemented in PSIM[®] software.

A. The Case of Constant Voltage Reference v_{ref}

Two different but symmetric output voltage references $v_{\text{ref}} = 10/7$ V ($V_o = 10$ V) and $v_{\text{ref}} = -10/7$ V ($V_o = -10$ V) were selected. According to (6), their corresponding steady-state duty cycles are $D = 0.755$ and its complementary value $D = 0.245$. In order to explore the dependence of the system dynamic behavior in terms of its parameters, the proportional gain has been selected as the parameter to be varied. The results are depicted in Fig. 6 where the waveforms of the state variables and the control signals just before and after subharmonic oscillation takes place are shown. The results show that for both $D = 0.755$ and its complementary value $D = 0.245$, the critical value of the proportional gain is $k_p \approx 11.1$. This value is in a very good agreement with the theoretical results from the closed-form condition (18) plotted in Fig. 5 and the numerically computed bifurcation diagrams depicted in Fig. 3.

B. The Case of Sinusoidal Voltage Reference v_{ref}

Fig. 7 shows the waveforms of the state variables and the control signals of the system before and after subharmonic oscillation takes place in the dc-ac H-bridge inverter with a sinusoidal reference voltage $v_{\text{ref}} = V_{\text{ref}} \sin(\omega_l t)$. Subharmonic oscillations starts appearing in some switching cycles at a value of $k_p \approx 8.3$. By increasing k_p , the number of switching cycles during which this phenomenon appear increases.

In order to show the effect of subharmonic oscillation on the system performance metrics, different tests have been performed for the three modulation schemes LEM, TEM and DEM and the results are summarized in Table III for the set of parameter values depicted in Table II and for $k_p = 9$. The voltage THD is limited within 0.6% for the case of the DEM while it is much higher in the case of the LEM and TEM schemes for the same set of parameter values.

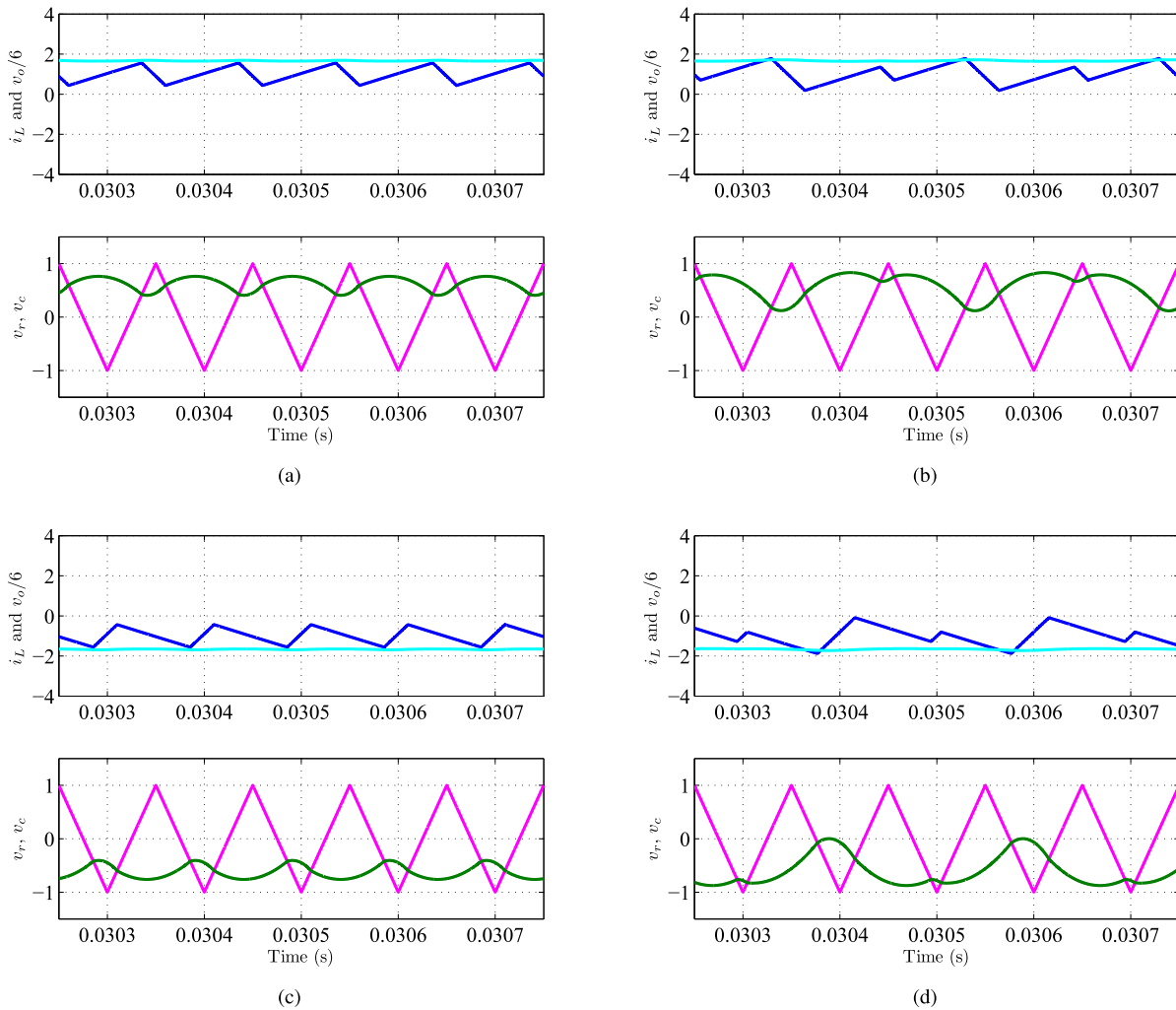


Fig. 6. PSIM[®] simulation showing the time-domain waveforms of the state variables and the control signals just before and after subharmonic oscillation takes place for two symmetric values of the duty cycles corresponding to average output voltage $V_o = -10$ V and $V_o = +10$ V. Left: $k_p = 11$, the system is stable. Right: $k_p = 11.2$, the system exhibits subharmonic oscillation. (a) $k_p = 11$ and $D = 0.755$. (b) $k_p = 11.2$ and $D = 0.755$. (c) $k_p = 11$ and $D = 0.245$. (d) $k_p = 11.2$ and $D = 0.245$.

TABLE III

THE PERFORMANCE METRICS FOR THREE DIFFERENT MODULATION STRATEGIES FROM NUMERICAL SIMULATIONS FOR $k_p = 9$

	LEM	TEM	DEM
Subharmonics	yes	yes	no
voltage THD	4%	3%	0.6%

VI. EXPERIMENTAL VALIDATION

An experimental prototype of an H-bridge inverter, using the parameters shown in Table II, has been built. The schematic of the experimental prototype is shown in Fig. 8. The power stage is made up of an H-bridge circuit, employing four W45NM50 MOSFETs with the driver IRS21834. Two identical radial inductors 1433428C from Murata Power Solutions whose nominal values are $330 \mu\text{H} \pm 10\%$ were connected in the top and the bottom sides of the H-bridge inverter. Their dc resistance was measured to be approximately $r_L = 0.1 \Omega$. A film capacitor whose capacitance value is $68 \mu\text{F}$ was placed in parallel with the output load resistance. The ESR of the capacitor was measured to be 0.1Ω . The voltage error

is processed by a PI controller implemented using standard OA devices shown in Fig. 8. The output of this controller is compared with a 10 kHz triangular signal provided from the signal generator Tektronix AFG2021. The results shown below were measured by using the oscilloscope Tektronix MDO3014 and the probes TEKTRONIX TPP0250 for illustrating the current waveforms.

The integrator proportional gain is selected as the parameter to be varied to explore the possible dynamical behaviors that the system could exhibit. First, it has been checked experimentally that the stability boundary is symmetric with respect to $D = 0.5$ and that the behavior of the system is the same for two different complementary steady-state values of the duty cycle D . Fig. 9 shows the control signals and the state variables for $D = 0.755$ ($V_o = 10$ V) and $D = 0.245$ ($V_o = -10$ V) confirming the previous claims concerning this symmetry. Next, the results corresponding to a sinusoidally time varying voltage reference will be presented.

As stated previously, in dc-ac applications, the reference voltage is a time varying sinusoidal signal and accordingly

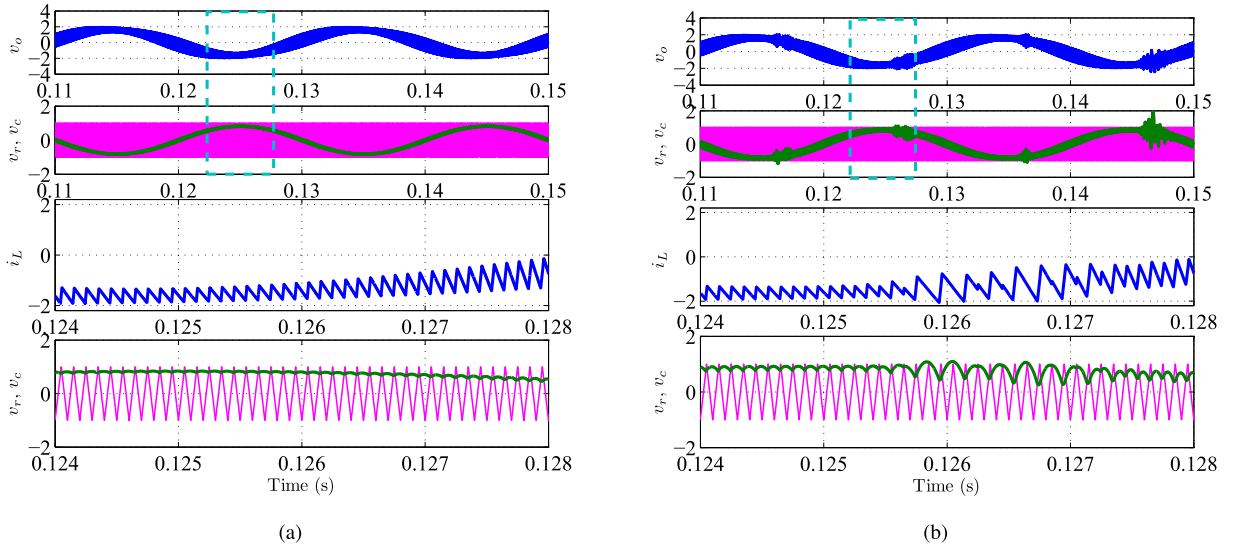


Fig. 7. Steady-state time-domain waveforms from PSIM[®] simulations before (a) and after (b) losing stability of the H-bridge converter with sinusoidal reference voltage v_{ref} with amplitude $V_{ref} = 2.2875$ V ($V_o = 16$ V). (a) the system is stable during the complete line cycle. (b) subharmonic oscillation starts taking place during some switching cycles. Increasing k_p further, subharmonic oscillation and chaotic regimes occupy more switching cycles.

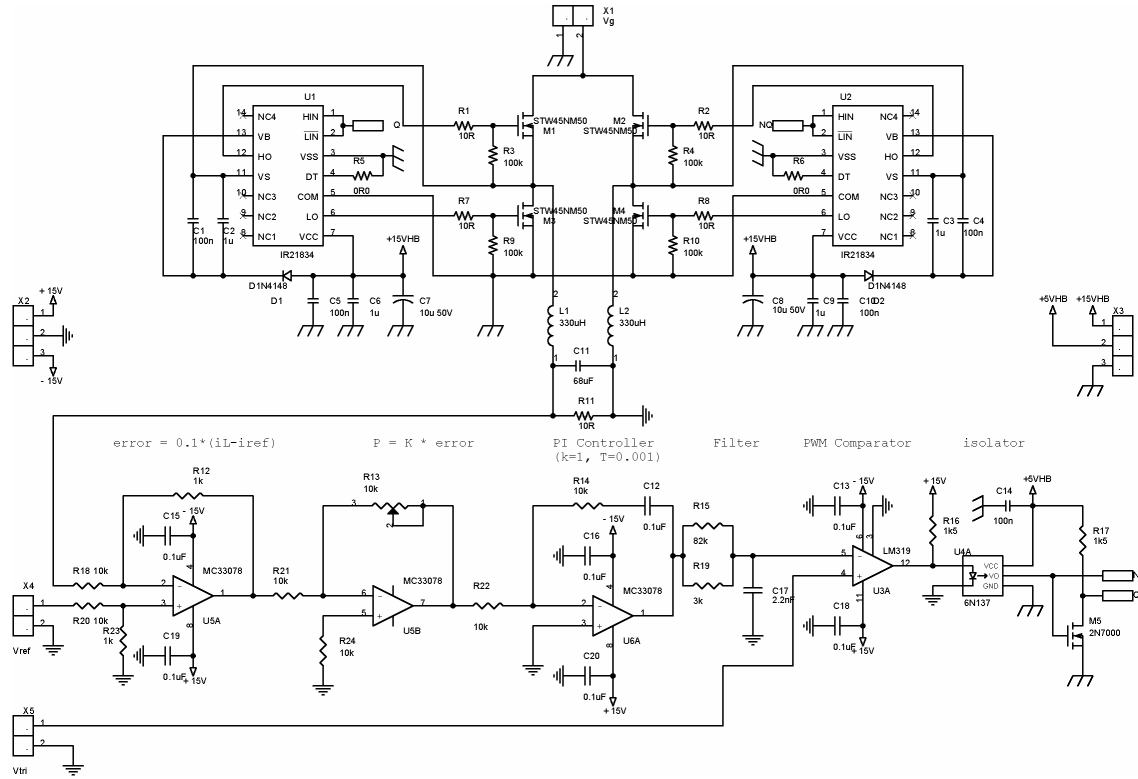


Fig. 8. Schematic circuit diagram of the experimentally implemented circuit for performing laboratory measurements.

the steady-state quasi-static duty cycle D_ϕ is given by (23). In such a situation, the phase ϕ is a quasi-static parameter like D_ϕ . One way to show the dynamic of the system along one half line cycle is by considering the phase ϕ as a slowly time varying parameter and perform the stability analysis in terms of this parameter together with other suitable parameters [19].

The stability boundary of the system is plotted in Fig. 10, in terms of the PI controller gain k_p and the phase angle

$\phi \in (0, \pi)$. In [19] such a plot has been obtained using numerical simulations from the switched model. Here, the plot in Fig. 10 is predicted from the closed-form expressions (18) and (23). The results from the numerical and experimental measurements are shown in the same plot. For estimating the experimental boundary and because of the non-stationarity of the experimental waveforms, for each value of the proportional gain, six different line cycles have been used to detect

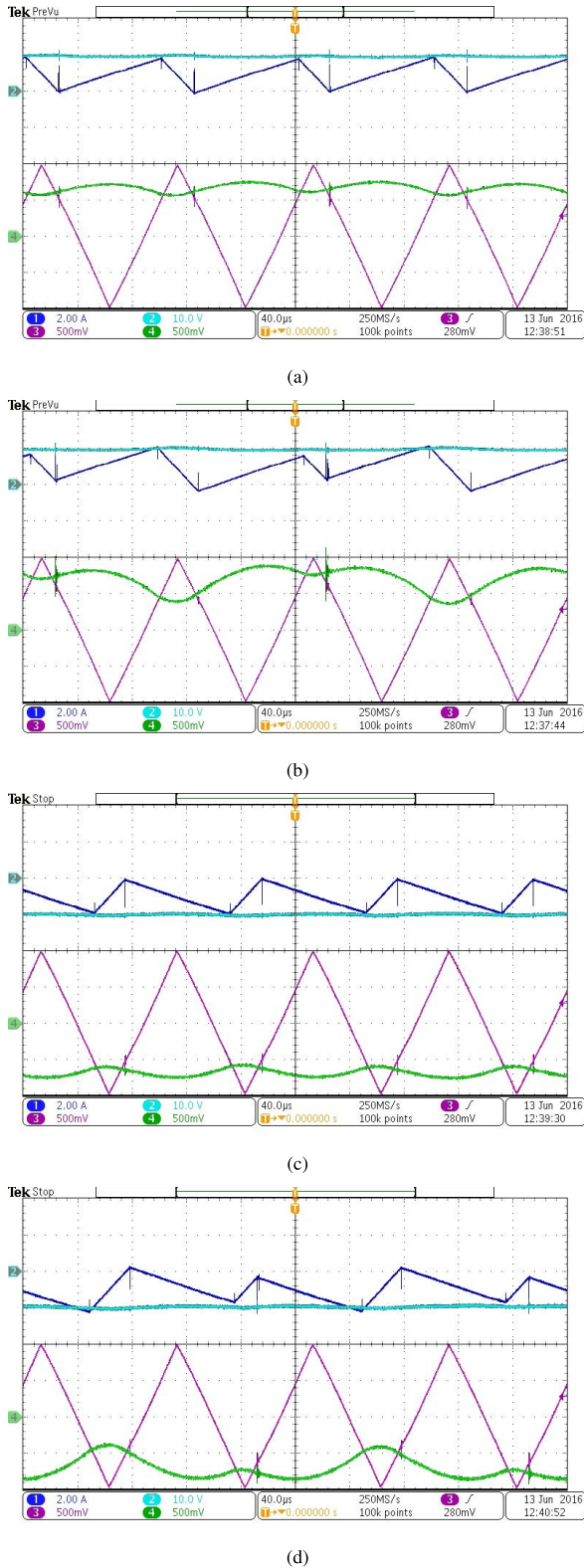


Fig. 9. Experimental waveforms of the state variables and the control signals just before and after subharmonic oscillation takes place for two symmetric values of the duty cycles corresponding to average output voltage $V_o = -10$ V and $V_o = +10$ V. (a) and (c): the system is stable. (b) and (d) the system exhibits subharmonic oscillation.

the critical phase where subharmonic oscillation starts to be exhibited.

Inside the region delimited by the curves, subharmonic oscillation takes place. This region gets wider when the

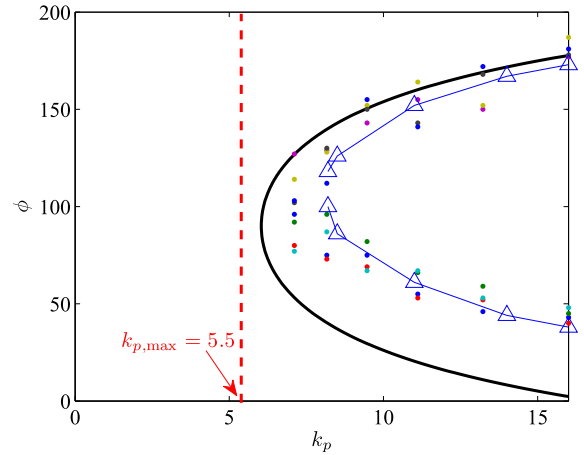


Fig. 10. Stability boundary of the H-bridge dc-ac inverter in terms of the phase angle ϕ and the PI controller gain k_p for $V_M = 2$ V. Solid curve: theoretical result from (18), Δ PSIM simulations. The cloud of points stand for the experimental results.

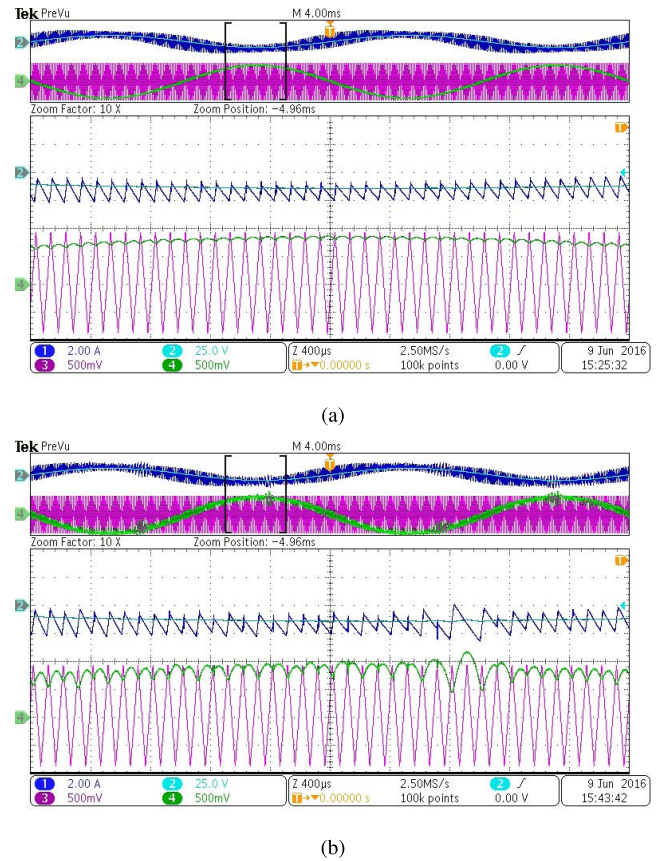


Fig. 11. Experimental waveforms (a) before and (b) after losing stability of the H-bridge converter with sinusoidal reference voltage v_{ref} . $V_M = 2$ V.

proportional gain k_p increases. At the left side of this region, the system exhibits stable operation during the entire line cycle. Since an expression of the theoretical critical value $k_{p,max}$ of the PI controller gain ensuring stability during the entire line cycle is available, this can be used as a safe value to get a system free from subharmonic oscillations. Vertical dashed line in Fig. 10 indicates this theoretical critical value

TABLE IV

THE PERFORMANCE METRICS FOR THREE DIFFERENT MODULATION STRATEGIES FROM EXPERIMENTAL MEASUREMENTS

	LEM	TEM	DEM
Subharmonics	yes	yes	no
voltage THD	4.5%	3.1%	0.9%

for the set of parameter values shown in Table II. Both (19) and (22) can be used to determine this value and no significant difference is noticed. Fig. 11 shows the steady-state response of the system obtained from experimental measurements using the experimental prototype of the dc-ac H-bridge inverter.

For $k_p = 3$, the system is stable during the entire line cycle because $k_p < k_{p,\max}|_{V_M=2} \approx 5.5$. Let us select $k_p = 9$. The system exhibits subharmonic oscillation at a certain phase angle $\phi_1 \approx 90^\circ$ in a close agreement with the theoretical value $\phi_1 \approx 83^\circ$ in Fig. 10. The other critical phase angle during the same half line cycle is $\phi_2 \approx 131^\circ$. Its estimate value is $\phi_2 \approx 180 - \phi_1 \approx 98^\circ$ as reported in [20]. This estimate value differs slightly from the theoretical value in Fig. 10. The discrepancies between the theoretical analysis and the simulation results can be attributed to the use of the quasi static approximation. The discrepancies with the experimental results can be attributed to the non-modeled dynamics and the non considered parasitic parameters. Different experimental tests have been performed for the three modulation schemes LEM, TEM and DEM and the results are summarized in Table IV for the set of parameter values depicted in Table II and for $k_p = 8$. As it can be observed, like for numerical simulation tests, the DEM strategy outperforms the LEM and TEM schemes in terms of stability and also power quality.

VII. CONCLUSIONS

This paper has focused on subharmonic oscillation boundary in single phase dc-ac H-bridge converters with double edge pulse width modulation strategy. In past studies, with this modulation strategy, subharmonic oscillation has merely been characterized by means of numerical simulations using either a discrete-time model, Floquet theory combined with the Filippov method or a switched system-level model. In this work an approximate closed-form expression for subharmonic oscillation occurrence has been derived. Based on the methodology presented, critical values of the system parameters are located accurately. The results reported here could help in selecting the parameter values of the system for avoiding subharmonic oscillation in a practical design, hence improving the power quality. A simple inspection of the expressions of the critical curves reveals the effect of the parameters on stability boundaries such as the amplitude of the triangular signal, the input voltage supply, the PI coefficients, the output load, the switching frequency, the inductance of the inductor and finally, the output capacitor. The conclusions obtained from the closed-form expression are confirmed using numerical simulations from PSIM[®] software. An experimental validation has been provided using a hardware prototype of an H-bridge inverter. Future works will deal with the extension of the approach used in this paper to more complex

dc-ac inverter topologies such as multi-level structures as well as to ac-dc power factor correction circuits. Exploration of the results for designing advanced controllers that can avoid these instabilities, taking into account communication delays and load nonlinearities is also a subject of further investigation.

REFERENCES

- [1] D. Giaouris, S. Banerjee, B. Zahawi, and V. Pickert, "Stability analysis of the continuous-conduction-mode buck converter via Filippov's method," *IEEE Trans. Circuits Syst. I, Reg. Papers*, vol. 55, no. 4, pp. 1084–1096, May 2008.
- [2] B. Robert and C. Robert, "Border collision bifurcations in a one-dimensional piecewise smooth map for a PWM current-programmed H-bridge inverter," *Int. J. Control*, vol. 75, nos. 16–17, pp. 1356–1367, 2002.
- [3] S. Akatsu, H. Torikai, and T. Saito, "Zero-cross instantaneous state setting for control of a bifurcating H-bridge inverter," *Int. J. Bifurcation Chaos*, vol. 17, no. 10, pp. 3571–3575, 2007.
- [4] L. Cheng, W.-H. Ki, F. Yang, P. K. T. Mok, and X. Jing, "Predicting subharmonic Oscillation of voltage-mode switching converters using a circuit-oriented geometrical approach," *IEEE Trans. Circuits Syst. I, Reg. Papers*, vol. 64, no. 3, pp. 717–730, Mar. 2017.
- [5] A. El Aroudi, "Prediction of subharmonic oscillation in switching converters under different control strategies," *IEEE Trans. Circuits Syst. II, Exp. Briefs*, vol. 61, no. 11, pp. 910–914, Nov. 2014.
- [6] E. Rodriguez, A. El Aroudi, F. Guinjoan, and E. Alarcon, "A ripple-based design-oriented approach for predicting fast-scale instability in DC–DC switching power supplies," *IEEE Trans. Circuits Syst. I, Reg. Papers*, vol. 59, no. 1, pp. 215–227, Jan. 2012.
- [7] C. C. Fang, "Closed-form critical conditions of subharmonic oscillations for buck converters," *IEEE Trans. Circuits Syst. I, Reg. Papers*, vol. 60, no. 7, pp. 1967–1974, Jul. 2013.
- [8] A. El Aroudi, "A new approach for accurate prediction of subharmonic oscillation in switching regulators—Part I: Mathematical derivations," *IEEE Trans. Power Electron.*, vol. 32, no. 7, pp. 5651–5665, Jul. 2017.
- [9] F. Vasca and L. Iannelli, Eds., *Dynamics and Control of Switched Electronic Systems*. Heidelberg, Germany: Springer-Verlag, 2012.
- [10] R.-J. Wai and W.-H. Wang, "Grid-connected photovoltaic generation system," *IEEE Trans. Circuits Syst. I, Reg. Papers*, vol. 55, no. 3, pp. 953–964, Apr. 2008.
- [11] C.-Y. Yang, C.-Y. Hsieh, F.-K. Feng, and K.-H. Chen, "Highly efficient analog maximum power point tracking (AMPPT) in a photovoltaic system," *IEEE Trans. Circuits Syst. I, Reg. Papers*, vol. 59, no. 7, pp. 1546–1556, Jul. 2012.
- [12] T. A. Sakharuk, A. M. Stankovic, G. Tadmor, and G. Eirea, "Modeling of PWM inverter-supplied AC drives at low switching frequencies," *IEEE Trans. Circuits Syst. I, Fundam. Theory Appl.*, vol. 49, no. 5, pp. 621–631, May 2002.
- [13] K. Lee and J.-I. Ha, "Single-phase inverter drive for interior permanent magnet machines," *IEEE Trans. Power Electron.*, vol. 32, no. 2, pp. 1355–1366, Feb. 2017.
- [14] R. Gupta and A. Ghosh, "Frequency-domain characterization of sliding mode control of an inverter used in DSTATCOM application," *IEEE Trans. Circuits Syst. I, Reg. Papers*, vol. 53, no. 3, pp. 662–676, Mar. 2006.
- [15] A. Kawamura, R. Chuarayapratip, and T. Haneyoshi, "Deadbeat control of PWM inverter with modified pulse patterns for uninterruptible power supply," *IEEE Trans. Ind. Electron.*, vol. IE-35, no. 2, pp. 295–300, May 1988.
- [16] R. Middlebrook and S. Cuk, "A general unified approach to modelling switching-converter power stages," in *Proc. IEEE Power Electron. Spec. Conf.*, Jun. 1976, pp. 18–34.
- [17] S. Chiniforoosh *et al.*, "Definitions and applications of dynamic average models for analysis of power systems," *IEEE Trans. Power Del.*, vol. 25, no. 4, pp. 2655–2669, Oct. 2010.
- [18] X. Liu, A. M. Cramer, and F. Pan, "Generalized average method for time-invariant modeling of inverters," *IEEE Trans. Circuits Syst. I, Reg. Papers*, vol. 64, no. 3, pp. 740–751, Mar. 2017.
- [19] M. Li, D. Dai, and X. Ma, "Slow-scale and fast-scale instabilities in voltage-mode controlled full-bridge inverter," *Circuits, Syst. Signal Process.*, vol. 27, no. 6, pp. 811–831, 2008.
- [20] J.-K. Wu, L.-W. Zhou, and W.-G. Lu, "A unified bifurcation control strategy for voltage source inverter," *Acta Phys. Sinica*, vol. 61, no. 21, p. 210202, 2012.

- [21] A. Elbkosh, D. Giaouris, B. Zahawi, V. Pickert, and S. Banerjee, "Control of bifurcation of DC/DC buck converters controlled by double-edged PWM waveform," in *Proc. ENOC*, Saint Petersburg, Russia, Jun./Jul. 2008, pp. 1–5.
- [22] A. El Aroudi, W. G. Lu, M. Al-Numay, and H. H. C. Iu, "Subharmonic instability boundary in DC-AC H-bridge inverters with double edge PWM," in *Proc. IEEE Int. Symp. Circuits Syst. (ISCAS)*, May 2015, pp. 2089–2092.
- [23] H. R. Baghaee, M. Mirsalim, G. B. Gharehpetian, and H. A. Talebi, "A generalized descriptor-system robust H_∞ control of autonomous microgrids to improve small and large signal stability considering communication delays and load nonlinearities," *Int. J. Elect. Power Energy Syst.*, vol. 92, pp. 63–82, Nov. 2017.
- [24] R. W. Erickson and D. Maksimovic, *Fundamentals of Power Electronics*, 2nd ed. New York, NY, USA: Springer, 2001.



Abdelali El Aroudi (M'00–SM'13) received the Degree in physical science from the Faculté des sciences, Université Abdelmalek Essaadi, Tetouan, Morocco, in 1995, and the Ph.D. degree (Hons.) in applied physical science from the Universitat Politècnica de Catalunya, Barcelona, Spain, in 2000. From 1999 to 2001, he was a Visiting Professor with the Department of Electronics, Electrical Engineering and Automatic Control, Technical School of Universitat Rovira i Virgili, Tarragona, Spain, where he became an Associate Professor in

2001 and a full-time tenure Associate Professor in 2005. His research interests are in the field of structure and control of power conditioning systems for autonomous systems, power factor correction, stability problems, nonlinear phenomena, chaotic dynamics, bifurcations and control. He is a Guest Editor of the IEEE JOURNAL ON EMERGING AND SELECTED TOPICS IN CIRCUITS AND SYSTEMS Special Issue on Design of Energy-Efficient Distributed Power Generation Systems in 2015. He currently serves as an Associate Editor in IEE *IET Power Electronics* and the IEE *IET Electronics Letters*.



Mohammed S. Al-Numay (M'04) was born in Riyadh, Saudi Arabia. He received the B.S. degree (Hons.) from King Saud University, Riyadh, Saudi Arabia, in 1986, the M.S. degree from Michigan State University, East Lansing, MI, USA, in 1990, and the Ph.D. degree from the Georgia Institute of Technology, Atlanta, GA, USA, in 1997, all in electrical engineering. Since 1998, he has been with the Electrical Engineering Department, King Saud University, where he is currently a Professor. From 2002 to 2006, he was the Dean of Admissions and

Registration, King Saud University. In 2017, he was appointed as the Vice Rector for Education and Academic Affairs in the same university. Since 2008, he has been a Senior Consultant of Student Information Systems and electronic admission to many governmental and private universities and colleges. His research interests include modeling, analysis, design, and control of power electronics.



Wei Guo Lu (M'14) received the B.S., M.S., and Ph.D. degrees in electrical engineering from Chongqing University, Chongqing, China, in 2000, 2003, and 2008, respectively. He is currently a Professor with the School of Electrical Engineering, Chongqing University, Chongqing, China. He is an author or co-author of more than 20 papers in journal or conference proceedings. His current research interests include the stability analysis and control strategies of switching power converters and magnetic-resonance wireless power transfer.



Josep Maria Bosque-Moncusí received the degree in industrial technical engineering, the master's degree in electronics engineering, and the Ph.D. degree from the Universitat Rovira i Virgili (URV), Tarragona, Spain, in 2005, 2009, and 2014, respectively. Since 2004, he has been a Research Technician with the Automatics and Industrial Electronics Research Group, URV. His research interests include power electronics for renewable energies and electrical vehicles. He is currently with Lear Corporation company, Tarragona, Spain.



Herbert Ho-Ching Iu (S'98–M'00–SM'06) received the B.Eng. degree (Hons.) in electrical and electronic engineering from The University of Hong Kong, Hong Kong, in 1997, and the Ph.D. degree in electronic and information engineering from The Hong Kong Polytechnic University, Hong Kong, in 2000. In 2002, he joined the School of Electrical, Electronic and Computer Engineering, The University of Western Australia, where he is currently a Professor. His research interests include power electronics, renewable energy, nonlinear

dynamics, current sensing techniques, and memristive systems. He received the IET Power Electronics Premium Award, the IET Generation, Transmission and Distribution Premium Award and the UWA Vice-Chancellor Mid-Career Research Award, and the IEEE PES Western Australian Chapter Outstanding Engineer Award in 2012, 2014, and 2015, respectively. He currently serves as an Editor for the IEEE TRANSACTIONS ON SMART GRIDS, an Associate Editor for the IEEE TRANSACTIONS ON POWER ELECTRONICS, the IEEE TRANSACTIONS ON NETWORK SCIENCE AND ENGINEERING, the IEEE TRANSACTIONS ON CIRCUITS AND SYSTEMS-II, and the IEEE ACCESS.